

Final Project for Computational Models in Biology: Modeling TF Dynamics in Pluripotency and Cancer

Nitay Amiel

April 7, 2025

1 Introduction

Stem cells are a unique class of cells characterized by their ability to both self-renew and differentiate into various specialized cell types. These capabilities are critical during embryonic development, tissue regeneration, and cellular homeostasis. Pluripotent stem cells, such as embryonic stem cells (ESCs), are capable of giving rise to all three germ layers—ectoderm, mesoderm, and endoderm—and thereby contribute to the formation of every tissue in the body [8].

The regulation of stem cell pluripotency is controlled by a tightly regulated transcriptional network. At the core of this network lie three master transcription factors (TFs): OCT4, SOX2, and NANOG. These TFs function cooperatively in a feedback and feedforward loop structure that reinforces pluripotency and represses differentiation [1]. OCT4 and SOX2 form a heterodimer that activates the expression of NANOG and each other. In turn, NANOG reinforces its own expression and positively regulates OCT4 and SOX2. This triad forms a bistable genetic switch governing stem cell fate.

To quantitatively describe the regulatory interactions among these transcription factors, the Shea-Ackers formalism is often employed. This thermodynamic approach models transcriptional regulation based on the binding affinities of transcription factors to promoter regions and the probabilities of different binding configurations. In the context of NANOG, SOX2, and OCT4, the Shea-Ackers model allows for calculating the probabilities of promoter activation as a function of TF concentrations and cooperative binding—capturing how the formation of OCT4-SOX2 heterodimers and NANOG feedback drive expression states that define pluripotency.

In addition to transcriptional regulation, post-translational modifiers (PTMs) play a critical role in modulating the stability, localization, and activity of these key transcription factors. PTMs such as phosphorylation, acetylation, and ubiquitination can degrade the functional output of NANOG, SOX2, and OCT4 in response to signaling cues, enabling changes in stem cell behavior. These modifications are essential for fine-tuning the pluripotency network and ensuring robust yet flexible control of stem cell fate decisions [5].

Beyond embryogenesis, recent studies have implicated aberrant expression of OCT4, SOX2, and NANOG in various cancers, including oral squamous cell carcinoma (OSCC). The expression of these TFs has been observed not only in ESCs but also in premalignant

and malignant oral tissues [3]. Their presence in oral cancer suggests that the molecular machinery normally responsible for maintaining stem cell pluripotency is co-opted during oncogenesis to promote the uncontrolled self-renewal and maintenance of undifferentiated, stem-like cancer cells.

2 Motivation

Given the evidence for the aberrant expression of the transcription factors OCT4, SOX2, and NANOG in certain oral cancer cells, this project aims to investigate conditions under which a cell exhibiting a stable pluripotent (ON) state can be driven toward a differentiated (OFF) state. In our model, the OFF state is characterized by a relatively low steady-state concentration of NANOG.

To achieve this, we focus on a negatively acting regulatory signal, denoted as B^- , which reduces the transcription rate of NANOG. This signal may represent, for instance, the action of p53 or other differentiation-promoting factors. Our objective is to determine the range of B^- signal levels that are sufficient to transition the system from ON to OFF.

We pursue this goal using two complementary approaches. First, we analyze the system deterministically to identify the critical threshold value of B^- above which the system reliably transitions to the OFF state. Second, we examine the system stochastically, focusing on behavior in the neighborhood of this threshold to determine whether intrinsic fluctuations can induce OFF transitions even at sub-threshold levels of B^- . This exploration may reveal whether the inherent stochastic nature of gene regulation can assist in suppressing the pluripotent state, offering potential biological or therapeutic insights.

Our study applies this investigative procedure across three different cellular environments, each representing a distinct mechanism that could influence the system’s sensitivity to the B^- signal:

1. **Baseline environment:** We begin with the standard model described in [1], which captures the dynamics of the core transcriptional network involving OCT4, SOX2, and NANOG. This serves as our reference case for threshold analysis and stochastic behavior.
2. **Enhanced PTM presence:** Given the crucial role of post-translational modifications (PTMs) in regulating transcription factors [5], we extend the model to include increased activity of a specific PTM. In our implementation, we simulate elevated levels of WWP2, an E3 ligase, which promotes ubiquitination and degradation of OCT4 [4]. We then analyze whether this enhanced PTM activity reduces the necessary B^- signal level required to deactivate the system.
3. **Reduced OCT4-SOX2 binding affinity:** Lastly, we consider a cellular environment in which the binding affinity between OCT4 and SOX2 is diminished—whether due to external factors such as molecular inhibitors or altered physicochemical conditions (e.g., high temperature). Since the OCT4-SOX2 heterodimer plays a central role in sustaining NANOG expression, reducing its formation is expected to weaken

the network’s self-sustaining feedback. We investigate how this change alters the B^- threshold and affects stochastic suppression behavior.

By systematically analyzing the system under these conditions, both deterministically and stochastically, we aim to uncover potential mechanisms by which the pluripotency network may be destabilized—thus providing a framework for understanding how cancer-associated stem-like states might be therapeutically targeted.

3 Model Formulation

3.1 Reaction Scheme

Figure 1 provides a high-level schematic of the regulatory network, capturing both transcriptional regulation and protein–protein binding interactions among the core factors.

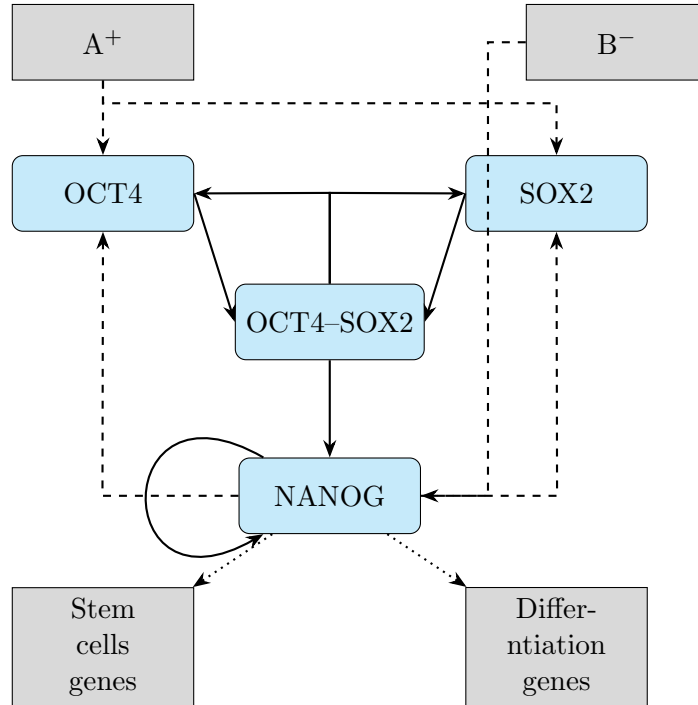
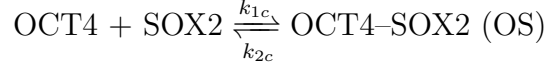
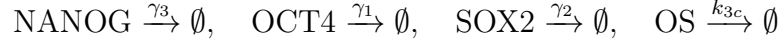


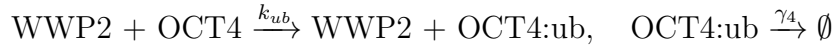
Figure 1: Stem cell transcriptional network showing regulation by A^+ and B^- , and the core loop among OCT4, SOX2, and NANOG. Solid arrows represent binding interactions or transcriptional activation; dashed arrows indicate transcriptional regulation without binding; and dotted arrows denote downstream expression outcomes. A^+ stimulates OCT4 and SOX2, while B^- negatively regulates NANOG.

The transcriptional regulation in this system is modeled using the Shea–Ackers thermodynamic framework, which allows us to express promoter occupancy as a function of transcription factor binding configurations and concentrations. The full transcriptional dynamics for OCT4, SOX2, and NANOG are detailed in the equations section and follow the formulation in [1, 2].

Here, we outline the remaining baseline reactions in the system, excluding transcription-related terms. These include degradation and complex formation processes:



In the cell type representing WWP2 presence (described as Type 2 in the Motivation section), we add additional reactions relating to ubiquitination:



3.2 Differential Equations

The differential equations describing the dynamics of each species in the baseline model consist of one term related to transcription—modeled using the Shea–Ackers approach, fully detailed in [1]—and additional terms representing degradation and binding reactions, as outlined above:

$$\begin{aligned} \frac{d[O]}{dt} &= \frac{\eta_1 + a_1[A_+] + a_2[OS] + a_3[OS][N]}{1 + \eta_2 + b_1[A_+] + b_2[OS] + b_3[OS][N]} - \gamma_1[O] - k_{1c}[O][S] + k_{2c}[OS] \\ \frac{d[S]}{dt} &= \frac{\eta_3 + c_1[A_+] + c_2[OS] + c_3[OS][N]}{1 + \eta_4 + d_1[A_+] + d_2[OS] + d_3[OS][N]} - \gamma_2[S] - k_{1c}[O][S] + k_{2c}[OS] \\ \frac{d[OS]}{dt} &= k_{1c}[O][S] - k_{2c}[OS] - k_{3c}[OS] \\ \frac{d[N]}{dt} &= \frac{\eta_5 + e_1[OS] + e_2[OS][N]}{1 + \eta_6 + f_1[OS] + f_2[OS][N] + f_3[B_-]} - \gamma_3[N] \end{aligned}$$

In the cell type representing WWP2 presence (described as Type 2 in the Motivation section), the ODE for OCT4 includes an additional degradation term due to ubiquitination:

$$\frac{d[O]}{dt} = \frac{\eta_1 + a_1[A_+] + a_2[OS] + a_3[OS][N]}{1 + \eta_2 + b_1[A_+] + b_2[OS] + b_3[OS][N]} - \gamma_1[O] - k_{1c}[O][S] + k_{2c}[OS] - \mathbf{k}_{ub}[\text{WWP2}][O]$$

3.3 Parameter Values

For the baseline model, we adopt the numerical values reported in [1] and documented in [2]:

η_1	a_1	a_2	a_3	η_2	b_1	b_2	b_3	η_3	c_1	c_2	c_3
10^{-4}	1	0.01	0.2	10^{-7}	0.0011	0.001	0.0007	10^{-4}	1	0.01	0.2
η_4	d_1	d_2	d_3	η_5	e_1	e_2	η_6	f_1	f_2	f_3	k_{1c}
10^{-7}	0.0011	0.001	0.0007	10^{-4}	0.005	0.1	10^{-7}	0.001	$9.95 \cdot 10^{-4}$	0.01	0.05
k_{2c}	k_{3c}	$[A_+](\text{ON})$	γ_1	γ_2	γ_3						
0.001	5	100	1	1	1						

Time is measured in seconds, and concentrations in nanomolar (nM).

WWP2-Present Cell Type (Type 2): To model the presence of the WWP2 E3 ligase, we use results from [6]. As shown in Figure 7C of that work, WWP2 expression causes approximately a 70% decrease in OCT4 transcriptional activity. Based on this, we estimate the additional degradation term due to ubiquitination as:

$$k_{ub} = 2.5 \times k_{deg}^{\text{OCT4}} = 2.5 \times \gamma_1 = 2.5 \times 1 = 2.5$$

We assume the same degradation rate and initial concentration for WWP2 as used for other species:

$$[WWP2] = 0.25, \quad \gamma_4 = 1$$

Reduced Binding Affinity (Type 3): To simulate reduced binding affinity between OCT4 and SOX2, we refer to [7], where Figure 2B demonstrates that the SOX2 S113 mutant decreases complex formation and reprogramming efficiency by a factor of 2. Based on this, we adjust the rate constants for complex formation and dissociation as follows (decreasing the binding and disassociation rates by 25% each):

$$k_{1c}^{\text{new}} = 0.75 \times k_{1c}^{\text{old}}, \quad k_{2c}^{\text{new}} = 1.25 \times k_{2c}^{\text{old}}$$

3.4 Model Assumptions

To simplify the system while preserving core regulatory behavior, we base our model on the following key assumptions:

- **The concentrations of external signals A^+ and B^- are constant over time**, representing fixed environmental inputs or upstream regulatory control.
- **All species are uniformly distributed in a well-mixed environment**, neglecting spatial effects or cellular compartmentalization.
- **Post-translational modification (PTM) effects are modeled phenomenologically**, by increasing the degradation rate of OCT4 to reflect WWP2-mediated ubiquitination. Similarly, in the reduced binding affinity model, the impact of inhibitory factors or mutations is modeled by adjusting the kinetic rates of OCT4–SOX2 complex formation and dissociation, without explicitly modeling inhibitor dynamics or molecular conformational changes.

4 Results

For each of the three model variants, we first determined the steady-state behavior of the system as a function of the B^- signal using deterministic simulations. The system of ODEs was solved numerically using MATLAB’s `ode45` solver, with initial conditions corresponding to the high NANOG ON state. This allowed us to identify the B^- threshold—the minimum inhibitory signal strength required to drive the system into the OFF state under deterministic conditions.

To assess the role of intrinsic noise, we then simulated the system stochastically near this threshold using the Gillespie algorithm. The stochastic simulation was run for a duration of 300 seconds, with 10 iterations performed for each B^- value to compute average trajectories. The goal was to estimate the *convergence radius*—the range below the deterministic threshold where fluctuations alone could drive the system to the OFF state. We defined the system as OFF if the NANOG concentration dropped below 0.2 nM, compared to its initial ON-state value of 64 nM.

A summary of the resulting threshold values and convergence radius is presented in Table 1, and the corresponding trajectory plots are provided in the supplementary file.

Model Variant	Deterministic Threshold for B^-	Convergence Radius to OFF (Stochastic)
Baseline model	36	~ 10
Addition of a PTM	17	~ 8
Reduced binding affinity	24	~ 6

Table 1: Comparison of deterministic and stochastic system responses across model variants.

5 Discussion

The results in Table 1 demonstrate that both enhanced PTM activity and reduced OCT4–SOX2 binding affinity significantly affect the system’s stability and its sensitivity to the B^- signal.

In the baseline model, a relatively high B^- signal threshold (36 nM) is required to shift the system from the ON to OFF state, reflecting the robustness of the core pluripotency loop. When WWP2-mediated ubiquitination of OCT4 is introduced, the threshold drops to 17 nM—indicating that post-translational regulation can facilitate destabilization of the self-renewal state. This aligns with experimental evidence that OCT4 degradation via PTMs is a critical step in exiting pluripotency.

Similarly, reducing the binding affinity between OCT4 and SOX2 increased the system’s susceptibility to repression, lowering the threshold to 24 nM. Since the OCT4–SOX2 complex is essential for NANOG activation, weakening this interaction compromises the feedback loop and promotes deactivation.

Stochastic simulations further reveal that fluctuations enable transitions to the OFF state even slightly below the deterministic threshold. Notably, the convergence radius was smallest in the reduced binding affinity model (~ 6 nM), indicating that this variant is the most

resistant to noise-driven switching. In other words, only when the B^- signal is relatively close to or exceeds the deterministic threshold does the system reliably transition to the OFF state. This suggests that weakened OCT4–SOX2 complex formation, while reducing the deterministic threshold, also stabilizes the system against random fluctuations.

These findings suggest that targeting post-translational modifiers (like WWP2) or interfering with TF dimerization could be viable strategies to suppress aberrant self-renewal in cancerous cells that hijack stemness programs.

However, the model simplifies many biological aspects. For instance, protein synthesis and degradation rates were held constant across conditions, and spatial regulation was ignored. Further studies could explore dynamic PTM pathways, cooperative TF binding, or spatial heterogeneity in signaling.

References

- [1] Chickarmane, V., Troein, C., Nuber, U. A., Sauro, H. M., & Peterson, C. (2006). Transcriptional dynamics of the embryonic stem cell switch. *PLoS Computational Biology*, **2**(9), e123. <https://journals.plos.org/ploscompbiol/article?id=10.1371/journal.pcbi.0020123>
- [2] Chickarmane, V., Troein, C., Nuber, U. A., Sauro, H. M., & Peterson, C. (2006). Supplementary Text S1: Transcriptional Dynamics of the Embryonic Stem Cell Switch. *Supporting Information for PLoS Computational Biology*, **2**(9):e123. <https://journals.plos.org/ploscompbiol/article/file?type=supplementary&id=10.1371/journal.pcbi.0020123.sd001>
- [3] Swain, N., Thakur, M., Pathak, J., & Swain, B. (2020). SOX2, OCT4 and NANOG: The core embryonic stem cell pluripotency regulators in oral carcinogenesis. *Journal of Oral and Maxillofacial Pathology*, **24**(2), 368–373. <https://www.ncbi.nlm.nih.gov/pmc/articles/PMC7802841/>
- [4] Cai, N., Li, M., Qu, J., Liu, G.-H., & Izpisua Belmonte, J.C. (2012). Post-translational modulation of pluripotency. *Journal of Molecular Cell Biology*, **4**(4), 262–265. <https://academic.oup.com/jmcb/article/4/4/262/908451>
- [5] Cytoskeleton, Inc. (n.d.). Posttranslational regulation of key transcription factors in pluripotent stem cells. <https://www.cytoskeleton.com/posttranslational-regulation-of-key-transcription-factors-in-pluripotent-stem-cells>
- [6] Xu, H.M., Liao, B., Zhang, Q.J., Wang, B.B., Li, H., Zhong, X.M., Sheng, H.Z., Zhao, Y.X., Zhao, Y.M., Jin, Y. (2004). Wwp2, an E3 ubiquitin ligase that targets transcription factor Oct-4 for ubiquitination. *Journal of Biological Chemistry*, **279**(22), 23495–23503. [https://www.jbc.org/article/S0021-9258\(20\)66722-9/fulltext](https://www.jbc.org/article/S0021-9258(20)66722-9/fulltext)
- [7] Tapia, N., MacCarthy, C., Esch, D., Marthaler, A.G., Tiemann, U., Araújo-Bravo, M.J., Jauch, R., Cojocar, V., Schöler, H.R. (2015). Dissecting the role of distinct OCT4–SOX2 heterodimer configurations in pluripotency. *Scientific Reports*, **5**, 13533. <https://www.nature.com/articles/srep13533>

- [8] Zakrzewski, W., Dobrzynski, M., Szymonowicz, M., & Rybak, Z. (2019). Stem cells: Past, present, and future. *Stem Cell Research & Therapy*, **10**, Article 68. <https://stemcellres.biomedcentral.com/articles/10.1186/s13287-019-1165-5>